Palaeontology
The Palaeontological Association
www.palass.org

[Palaeontology, Vol. 63, Part 5, 2020, pp. 689–701]

POTENTIAL EVOLUTIONARY TRADE-OFF BETWEEN FEEDING AND STABILITY IN CAMBRIAN CINCTAN ECHINODERMS

by IMRAN A. RAHMAN[1], JAMES O'SHEA[2†], STEPHAN LAUTENSCHLAGER[3] *and* SAMUEL ZAMORA[4]

[1]Oxford University Museum of Natural History, Parks Road, Oxford, OX1 3PW, UK; imran.rahman@oum.ox.ac.uk
[2]School of Earth Sciences, University of Bristol, Wills Memorial Building, Queens Road, Bristol, BS8 1RJ, UK
[3]School of Geography, Earth & Environmental Sciences, University of Birmingham, Edgbaston, Birmingham, B15 2TT, UK; s.lautenschlager@bham.ac.uk
[4]Instituto Geológico y Minero de España, C/Manuel Lasala, 44, 9B, Zaragoza, 50006, Spain; s.zamora@igme.es

Typescript received 11 February 2020; accepted in revised form 17 April 2020

Abstract: Reconstructing the function and behaviour of extinct groups of echinoderms is problematic because there are no modern analogues for their aberrant body plans. Cinctans, an enigmatic group of Cambrian echinoderms, exemplify this problem: their asymmetrical body plan differentiates them from all living species. Here, we used computational fluid dynamics to analyse the functional performance of cinctans without assuming an extant comparative model. Three-dimensional models of six species from across cinctan phylogeny were used in computer simulations of water flow. The results demonstrate that cinctans with strongly flattened bodies produced much less drag than species characterized by dorsal protuberances or swellings, suggesting the former were more stable on the seafloor. However, unlike the flattened forms, cinctans with high-relief bodies were able to passively direct flow towards the mouth and associated food grooves, indicating that they were capable of more efficient feeding on particles suspended in the water. This study provides evidence of a previously unknown evolutionary trade-off between feeding and stability in Cambrian cinctan echinoderms.

Key words: echinoderm, cinctan, Cambrian, computational fluid dynamics, function, evolutionary trade-off.

THE sudden appearance of diverse animal phyla in the fossil record for the first time, a phenomenon known as the Cambrian explosion, is thought to represent one of the most significant events in the evolution of multicellular life. Elucidating the pattern of this fundamental evolutionary radiation has engendered considerable debate among palaeobiologists (e.g. Gould 1989; Conway Morris 1998; Marshall 2006; Erwin *et al.* 2011; Deline *et al.* 2018), in part due to the difficulty in interpreting the fossils that characterize this episode. To fully decode the evolutionary and biological significance of a fossil, an extant comparative model is normally required; however, many Cambrian taxa have body plans which are radically different to those of living animals, and hence the choice of interpretive model is problematic (Jenner & Littlewood 2008; Donoghue & Purnell 2009). Echinoderms are a case in point; several extinct Cambrian groups lack pentaradial symmetry and perhaps other synapomorphies of living echinoderms (Smith 2005, 2008; Zamora & Rahman 2014), and these fossil forms are therefore poorly understood.

Cinctans are one such group of aberrant early echinoderms, known exclusively from the Miaolingian Epoch of the Cambrian (*c.* 509–497 Ma) of Gondwana and Siberia (Smith & Zamora 2009; Zamora *et al.* 2013*a*). They are characterized by a flattened, asymmetrical body (theca), a rigid posterior appendage (stele), and an anterolateral mouth with one or an unequal pair of marginal food grooves (Fig. 1). Like all echinoderms, cinctans possess a calcite skeleton with a distinctive microstructure termed stereom, but they lack any trace of radial symmetry, a ubiquitous character of modern echinoderms; it is debated whether this absence is plesiomorphic (e.g. Smith 2005; Zamora & Rahman 2014) or derived (e.g. David *et al.* 2000). Moreover, it is unclear if they had an ambulacral system homologous to that of extant echinoderms (Parsley 1999; David *et al.* 2000; Smith 2005; Zamora & Smith 2008). The unusual character combination exhibited by cinctan fossils means they have no extant analogue, and hence many important details of their palaeobiology are controversial or unknown.

[†]Deceased

doi: 10.1111/pala.12495

To gain a better understanding of cinctan palaeobiology, Rahman *et al.* (2015*a*) used computational fluid dynamics (CFD) to investigate the functional performance of the cinctan *Protocinctus mansillaensis*. CFD is an approach for simulating fluid flows and their interaction with solid surfaces that is widely used in engineering, and which has emerged as a powerful tool in palaeontology (e.g. Rigby & Tabor 2006; Shiino *et al.* 2009, 2012; Bourke *et al.* 2014; Rahman *et al.* 2015*a*, *b*; Dynowski *et al.* 2016; Darroch *et al.* 2017; Waters *et al.* 2017; Wroe *et al.* 2018; Gibson *et al.* 2019; Gutarra *et al.* 2019). The method generates quantitative results based on numerical simulations of fluid flows, providing a rigorous framework for testing functional hypotheses in enigmatic fossil taxa without an extant analogue, such as cinctans. Rahman *et al.* (2015*a*) carried out CFD simulations of water flow for digital models of *P. mansillaensis* positioned at different orientations and burial depths in a virtual flume tank. Passive and active feeding scenarios were simulated by varying boundary conditions at the major body openings. The results showed that a position with the mouth facing downstream and the ventral swelling buried produced the least drag and lift, indicating this would have been beneficial for enhancing stability on the seafloor. In this position, flow to the mouth and associated marginal groove was minimal in simulations of passive suspension feeding, demonstrating that such a feeding mode would not have been an effective means of acquiring nutrients. In contrast, the simulations of active suspension feeding showed much stronger flow to the mouth and marginal groove, in agreement with previous interpretations of cinctans as pharyngeal filter feeders (Smith 2005; Zamora & Smith 2008). However, there is substantial morphological variation among cinctans, which exhibit varying degrees of asymmetry and thecal flattening (Smith & Zamora 2009; Zamora *et al.* 2013*b*), and therefore *P. mansillaensis* might not be a suitable model for the function and behaviour of the entire group.

Here, we used CFD to simulate fluid flow around three-dimensional digital models of six cinctans that encompassed the group's disparity (Fig. 2). These taxa included weakly to strongly asymmetrical forms, as well as species with and without dorsal protuberances or swellings. In this manner, we were able to analyse stability and feeding across cinctan phylogeny for the first time, shedding new light on the mode of life of this enigmatic extinct group.

MATERIAL AND METHOD

Box modelling

Three-dimensional (3-D) digital models of the cinctans *Graciacystis ambigua*, *Gyrocystis testudiformis*, *Lignanicystis barriosensis*, *Protocinctus mansillaensis*, *Trochocystites bohemicus* and *Undatacinctus quadricornuta* were constructed (Fig. 2). These species were selected because: (1) they provide a good representation of cinctan disparity; (2) they occupy a range of positions in cinctan phylogeny; and (3) their morphology is better known than that of other cinctans. Fossils of all six taxa were originally collected from fine-grained sedimentary rocks (shales or siltstones), which represent offshore marine

FIG. 1. Reconstruction of the cinctan *Protocinctus mansillaensis* in life position. Image: Óscar Sanisidro.

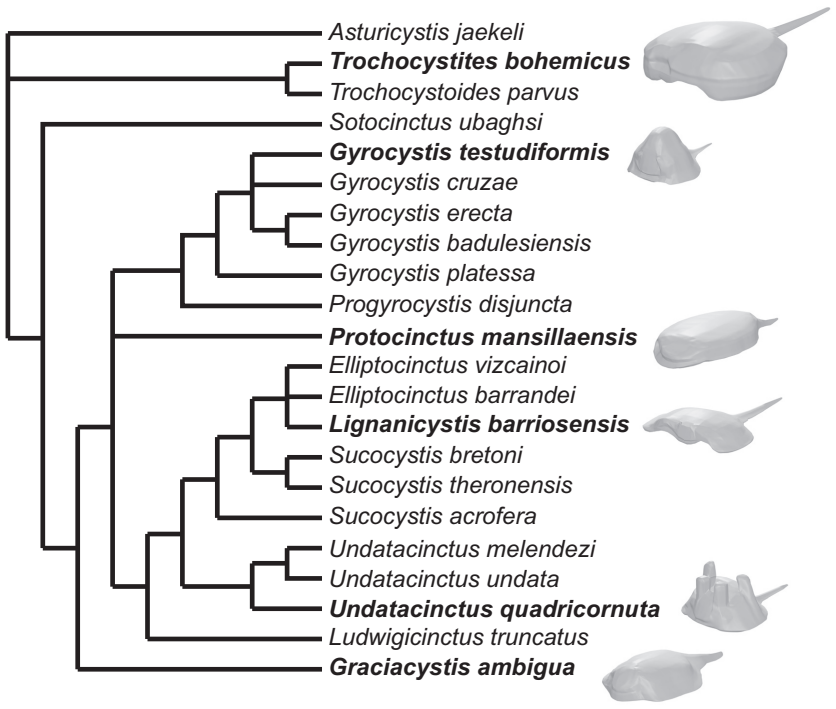

FIG. 2. Cinctan phylogeny with 3-D models of the six species included in the analysis. Phylogeny modified from Zamora *et al.* (2013*b*).

environments of low to moderate energy, sporadically affected by storms (Friedrich 1993; Álvaro & Vennin 1997; Zamora & Smith 2008; Rahman & Zamora 2009; Zamora & Álvaro 2010; Zamora *et al.* 2013*b*).

Two-dimensional reconstructions of the cinctans in multiple orientations (i.e. dorsal, ventral and frontal) were taken from the published literature (Friedrich 1993; Zamora & Smith 2008; Rahman & Zamora 2009; Zamora *et al.* 2013*b*), scaled to life size and used as reference images to guide box modelling (Rahman & Lautenschlager 2017) in Blender v. 2.75 (http://www.blender.org). The accuracy of these reference images was confirmed through first-hand observations of well-preserved fossil specimens, which helped to establish, for example, the height of the theca. A box-modelling approach was preferred over tomographic or surface-based methods because complete, articulated and three-dimensionally preserved fossil specimens are not available for the majority of cinctan taxa. It has been shown that box modelling can be used to create 3-D models that are almost identical to those derived from computed tomography or surface scanning of well-preserved fossil specimens and, moreover, these 3-D models generate very similar results in functional analyses (Rahman & Lautenschlager 2017), justifying our choice of methodology.

For each model, a primitive cube was used as a base object. First, the cube was subdivided to increase the number of elements. The vertices and edges of this object were then translated, rotated and scaled to fit the outline of the reference images in dorsal, ventral and frontal views. Additional elements were added in different orientations by extruding existing elements, thereby modelling other parts of the fossil. Finally, files were exported from Blender in STL format and converted into non-uniform rational basis spline (NURBS) surfaces (IGES format) in Geomagic Studio 2012 (http://www.geomagic.com). 3-D models in IGES format are available in Rahman *et al.* (2020).

Computational fluid dynamics

CFD simulations were carried out in COMSOL Multiphysics v. 5.3 (https://uk.comsol.com). The computational domain consisted of a 3-D half cylinder measuring 360 mm in length and 176 mm in diameter. Cinctan models were centrally fixed to the flat lower boundary of the half cylinder such that the domain extended at least three times the length of the fossil upstream, ten times the length of the fossil downstream and five times the size of the fossil in all other directions (Fig. 3A). This ensured the domain would be sufficiently large to allow the flow to fully develop on all sides of the model (Rahman 2017). Models were positioned with any ventral swellings below the lower boundary of the domain (equivalent to burial within the sediment) and with the mouth facing downstream (180° to the inlet), in agreement with previous studies of cinctan functional morphology (Friedrich 1993;

Jefferies *et al.* 1996; Parsley 1999; Zamora & Smith 2008; Rahman *et al.* 2015*a*). To explore the impact of orientation on our results, we repeated simulations for *T. bohemicus* with the model orientated at 0°, 45°, 90° and 135° to the inlet.

The physical properties of water (density = 1000 kg/m^3, dynamic viscosity = 0.001 Pa·s) were assigned to the domain surrounding the cinctan model. A normal inflow velocity inlet (velocity magnitude specified normal to boundary) was defined at the upstream end of the domain and a zero-pressure outlet (tangential stress component set to zero at boundary) was defined at the downstream end. Slip boundary conditions were assigned to the top and sides of the domain, allowing the fluid to pass along the walls without friction, and a no-slip boundary condition was assigned to the lower surface of the domain and the surfaces of the model, fixing the fluid velocity at zero (Fig. 3A). The domain was meshed using free tetrahedral elements, with thin layers of prismatic elements inserted along the interface between the fluid and solid surfaces to better capture the flow in this region (the boundary layer) (Fig. 3B, C). The Reynolds-averaged Navier–Stokes equations were solved using the shear-stress transport turbulence model; this uses a combination of the *k*-ω model in the boundary layer and the *k*-ϵ model in the freestream to give improved model performance (Menter 2009). A stationary solver was used to compute the steady-state flow patterns.

Ten inlet velocities ranging from 0.05 to 0.50 m/s (Reynolds numbers of 433–8215; width of the model in the flow taken as the characteristic dimension) were simulated for each cinctan model, thereby encompassing the typical range of near-bottom current velocities in modern storm-influenced marine settings (Puig *et al.* 2001; Valle-Levinson & Matsuno 2003). To evaluate the influence of the mesh on the results, we carried out a sensitivity analysis using different mesh sizes for each model.

The results of CFD simulations were quantified by computing drag forces (by integrating the total stress parallel to the flow direction), and the dimensionless coefficients of drag (C_D) were calculated using the following formula:

$$C_D = \frac{2F_D}{\rho U^2 A}$$

where F_D is the drag force exerted by the fluid (N), ρ is the density of the fluid (kg/m^3), U is the characteristic velocity (m/s) and A is the characteristic area (m^2). The projected frontal area was taken as the characteristic area. Additionally, CFD results were visualized as two-dimensional cross-sections of flow velocity magnitude with flow vectors. CFD simulation files in MPH format are available in Rahman *et al.* (2020).

RESULTS

Drag forces and coefficients

In our sensitivity analysis, we compared drag forces for different mesh sizes for each of the six cinctan models (Rahman *et al.* 2020, table S1). Results were considered mesh independent when the values were generally less than 2% different from those obtained with the next coarsest mesh. Based on these criteria, we selected a mesh for each model (ranging from 388 461 to 940 779 elements in size) that was used in all subsequent analyses.

In the simulations with *T. bohemicus* at different orientations, the drag forces and coefficients were lowest with the model orientated at 180° to the inlet; the drag coefficients were 6–39% higher at the other modelled orientations (Rahman *et al.* 2020, table S2). The drag forces were highest when the model was orientated at 45° to the inlet, whereas the drag coefficients were highest with the model orientated at 0°, 45° or 135° to the inlet (depending on the inlet velocity).

Comparing results for all six cinctan models orientated with the mouth facing downstream, the drag forces were highest for *U. quadricornuta*, followed by *T. bohemicus* and *Gy. testudiformis*, with *P. mansillaensis*, *L. barriosensis* and *Gr. ambigua* producing the lowest drag forces (Fig. 4; Rahman *et al.* 2020, table S3). The drag force increased as the inlet velocity increased, but the drag coefficient varied less consistently with velocity, increasing as the inlet velocity increased in *U. quadricornuta*, but decreasing as velocity increased in *Gr. ambigua*, *P. mansillaensis* and *T. bohemicus*. Moreover, in *Gy. testudiformis*, the drag coefficient increased with velocity up to 0.15 m/s, before decreasing steadily as the velocity increased up to 0.50 m/s, whereas in *L. barriosensis* the drag coefficient decreased as velocity increased up to 0.20 m/s, then increased with velocity up to 0.50 m/s. Similar to the drag forces, the drag coefficients were highest for *U. quadricornuta*, followed by *Gy. testudiformis*, with *P. mansillaensis*, *Gr. ambigua*, *T. bohemicus* and *L. barriosensis* producing the lowest drag coefficients for all simulated inlet velocities (Fig. 4; Rahman *et al.* 2020, table S3).

Flow patterns

In all cases, the velocity of the flow decreased as it approached the cinctan model and the lower boundary of the domain, with a steep velocity gradient developed close to the fluid–solid interface (the boundary layer). In addition, there was a region of low-velocity recirculating flow (the wake) immediately downstream of the model (Figs 5, 6; Rahman *et al.* 2020, figs S1–S13). Both the thickness of

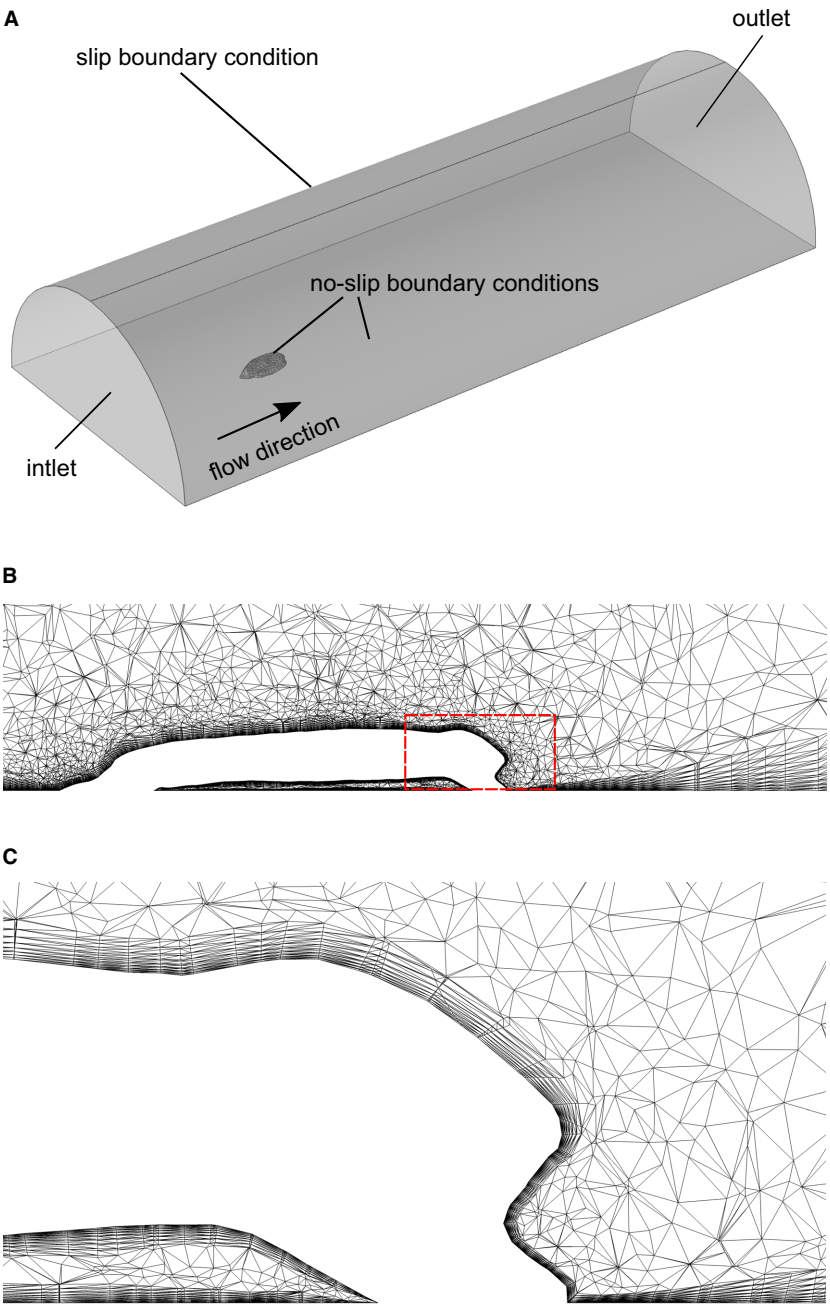

FIG. 3. A, computational domain used in CFD simulations. B–C, vertical cross-section through mesh used in CFD simulations for the cinctan *Protocinctus mansillaensis* (dashed box in B marks position of C). Modified from Rahman (2017). Colour online.

the boundary layer and the size of the wake decreased as the inlet velocity increased.

Flow patterns were substantially different depending on the orientation of *T. bohemicus* to the inlet. With the model orientated at 0° or 45° to the inlet, flow velocity around the mouth and adjacent food grooves was relatively high, governed by ambient flow rates (Rahman *et al.* 2020, fig. S1A, B). In contrast, when the model was orientated at 135° or 180° to the inlet, only low-velocity flow from within the wake was directed towards the mouth and food grooves (Rahman *et al.* 2020, fig. S1D, E). With the model orientated at 90° to the inlet, flow velocity around the mouth and food grooves was low and there was no recirculation to these parts of the model (Rahman *et al.* 2020, fig. S1C).

For the simulations with cinctan models orientated at 180° to the inlet, the extent to which flow within the wake was redirected to the mouth and food groove(s) varied between models. There was very little flow to these parts of the model in *Gr. ambigua* (Figs 5A, 6A; Rahman

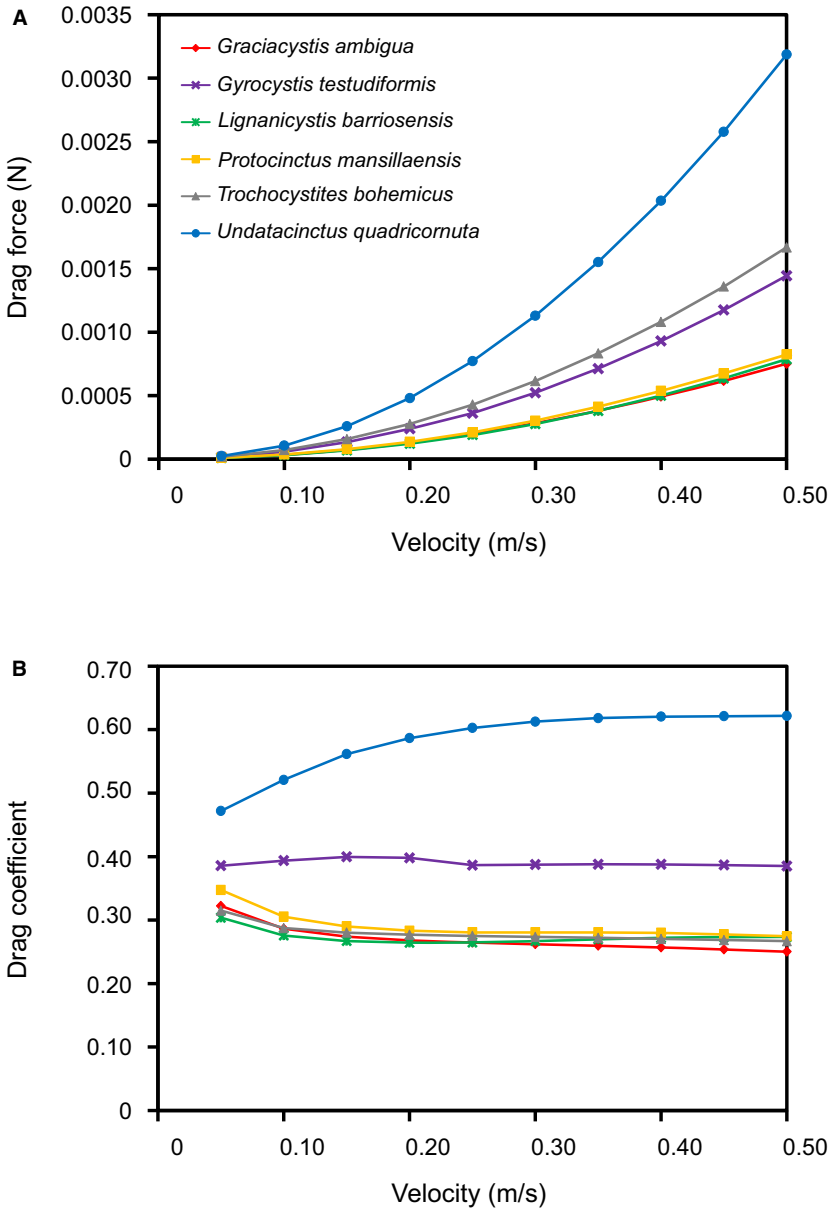

FIG. 4. Drag forces (A) and drag coefficients (B) for cinctan models.

et al. 2020, figs S2, S3), *L. barriosensis* (Figs 5C, 6C; Rahman *et al.* 2020, figs S6, S7) and *P. mansillaensis* (Figs 5D, 6D; Rahman *et al.* 2020, figs S8, S9), but generally much stronger recirculation in *Gy. testudiformis* (Figs 5B, 6B; Rahman *et al.* 2020, figs S4, S5), *T. bohemicus* (Figs 5E, 6E; Rahman *et al.* 2020, figs S10, S11) and *U. quadricornuta* (Figs 5F, 6F; Rahman *et al.* 2020, figs S12, S13). The shape of the wake ranged from approximately bilaterally symmetrical in *Gr. ambigua* and *P. mansillaensis* to more asymmetrical in *Gy. testudiformis*, *L. barriosensis*, *T. bohemicus* and *U. quadricornuta* (Fig. 5). In *L. barriosensis*, there was considerable flow underneath the model, through the two passageways in the ventral surface (Fig. 5C; Rahman *et al.* 2020, fig. S6).

FIG. 5. Two-dimensional plots (horizontal and vertical cross-sections) of flow velocity magnitude with flow vectors (size of arrows proportional to natural logarithm of flow velocity magnitude) at three different inlet velocities (0.10, 0.20, 0.50 m/s) for cinctan models. A, *Graciacystis ambigua*. B, *Gyrocystis testudiformis*. C, *Lignanicystis barriosensis*. D, *Protocinctus mansillaensis*. E, *Trochocystites bohemicus*. F, *Undatacinctus quadricornuta*. Position of mouth indicated by an asterisk (*). Direction of ambient flow from left to right.

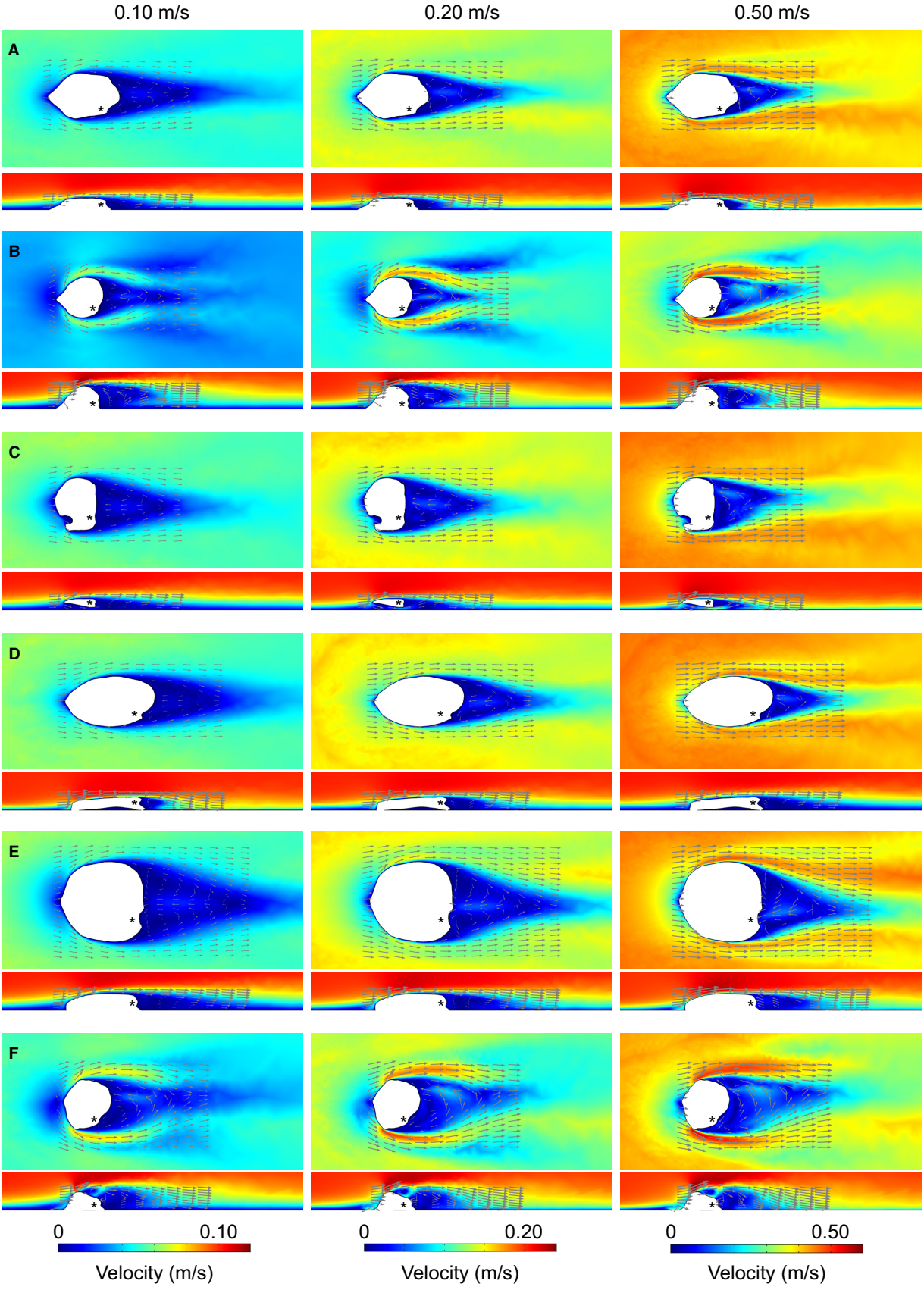
0.10 m/s
0.20 m/s
0.50 m/s
A
B
C
D
E
F
0
0.10
Velocity (m/s)
0
0.20
Velocity (m/s)
0
0.50
Velocity (m/s)

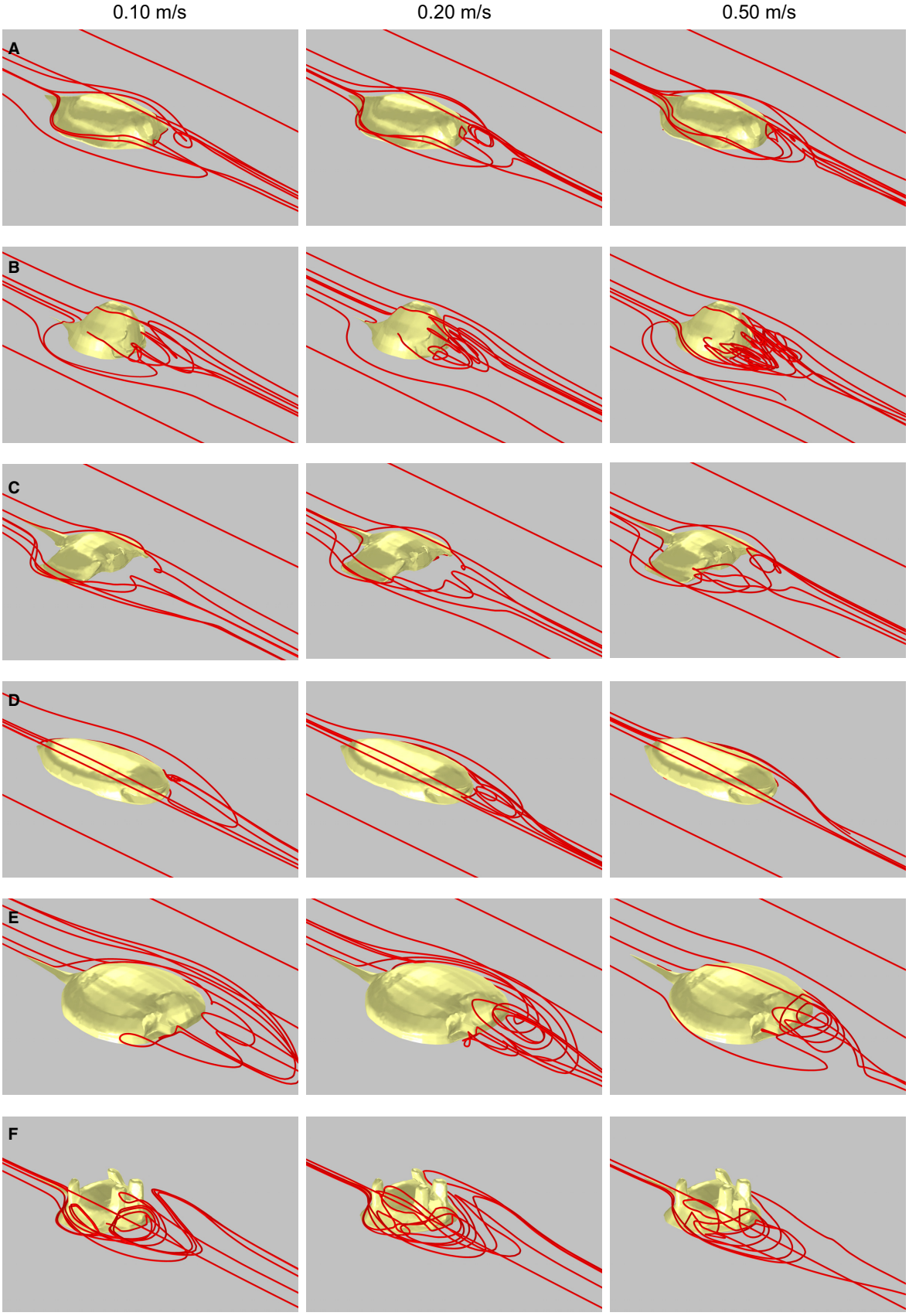
0.10 m/s
0.20 m/s
0.50 m/s
A
B
C
D
E
F

FIG. 6. Three-dimensional plots with streamlines at three different inlet velocities (0.10, 0.20, 0.50 m/s) for cinctan models. A, *Graciacystis ambigua*. B, *Gyrocystis testudiformis*. C, *Lignanicystis barriosensis*. D, *Protocinctus mansillaensis*. E, *Trochocystites bohemicus*. F, *Undatacinctus quadricornuta*. Direction of ambient flow from top left to bottom right. Colour online.

DISCUSSION

The CFD simulations show that the amount of drag generated by *T. bohemicus* varied with orientation, with the drag forces and coefficients lowest when it was orientated at 180° to the inlet (Rahman *et al.* 2020, table S2). Drag can be detrimental to the survival of modern epibenthic animals, making it difficult for them to remain in place upon the substrate (Koehl 1984, 1996; Vogel 1994), and it is likely that the same was true for cinctans, which lacked the complex attachment structures seen in many other Cambrian echinoderms (Zamora *et al.* 2017) and relied instead on the short stele and ventral swellings for anchoring to the seafloor (Ubaghs 1968; Friedrich 1993; Rahman & Zamora 2009). As a result, it is highly likely that *T. bohemicus* and other cinctans were preferentially orientated parallel to the current with the mouth facing downstream, thereby minimizing drag and enhancing stability on the seafloor (Rahman *et al.* 2015*a*). This position is also suggested by the flow patterns around *T. bohemicus* at different orientations; assuming cinctans fed by capturing particles suspended in water, as widely accepted (Ubaghs 1968; Friedrich 1993; Parsley 1999; David *et al.* 2000; Smith 2005; Zamora & Smith 2008), the lower flow velocities around the mouth and food grooves when *T. bohemicus* was orientated at 135° or 180° to the inlet (Rahman *et al.* 2020, fig. S1D, E) would be expected to have improved particle retention efficiency (Shimeta & Jumars 1991). Taken together, our results indicate that an orientation with the mouth facing downstream was optimal for both stability (through drag reduction) and feeding (through enhanced particle capture). To maintain this favourable position, cinctans would have needed to adjust their orientation as the current direction varied, perhaps by using small movements of the stele to re-orientate themselves, or by allowing themselves to be passively re-orientated by ambient currents, similar to some extant bryozoans, cnidarians and urochordates (Koehl 1976; Warner 1977; Young & Braithwaite 1980).

The drag forces and drag coefficients computed from the CFD simulations were also greatly influenced by the morphology of the modelled cinctans (Fig. 4; Rahman *et al.* 2020, table S3). *Undatacinctus quadricornuta*, which possessed well-developed projections on the dorsal surface, consistently produced the most drag of all the models included in the analysis. *Gyrocystis testudiformis*, which had a swollen dorsal integument, also generated substantial drag. In contrast, *Gr. ambigua*, *L. barriosensis* and *P. mansillaensis*, which were characterized by low relief, strongly flattened body shapes, produced the least drag. *Trochocystites bohemicus* produced the second highest drag forces, but among the lowest drag coefficients; this was a product of its considerably larger projected frontal area (up to more than double that of the other cinctans), which was taken as the reference area when calculating the drag coefficients. Consequently, we infer that the cinctans with flattened body shapes that minimized the drag coefficients (i.e. *Gr. ambigua*, *L. barriosensis*, *P. mansillaensis* and *T. bohemicus*) were less susceptible to dislodgement than high-relief forms like *Gy. testudiformis* and *U. quadricornuta*.

The recovered patterns of fluid flow were consistent with some existing interpretations of cinctan functional morphology (Friedrich 1993; Parsley 1999; Zamora & Smith 2008). For example, Zamora & Smith (2008) hypothesized that the ventral passageways in *L. barriosensis* would have allowed water flow under the theca, as observed in our results (Fig. 5C; Rahman *et al.* 2020, fig. S6). However, the CFD simulations also revealed flow patterns that had not been proposed previously, most strikingly the finding that there was considerable variation in the strength of recirculation downstream of the cinctan model depending on the height of the theca (Figs 5, 6; Rahman *et al.* 2020, figs S2–S13). Flow towards the mouth and food grooves was strongest when the thecal height was greater than 5 mm (i.e. *Gy. testudiformis* and *U. quadricornuta*) but minimal in the models that measured less than about 3 mm in height (i.e. *Gr. ambigua*, *L. barriosensis* and *P. mansillaensis*). In *T. bohemicus*, which was intermediate in height between these two sets of cinctans, flow to the mouth and food grooves was comparable in strength to that in *Gy. testudiformis* and *U. quadricornuta* when the inlet velocity was greater than 0.30 m/s, but more similar to *Gr. ambigua*, *L. barriosensis* and *P. mansillaensis* at lower velocities. This strongly suggests that high-relief forms would have had access to a greater supply of nutrients than low-relief ones.

It is debated whether cinctans were passive suspension feeders with a system of tentacles (Parsley 1999; David *et al.* 2000) or active pharyngeal filter feeders (Smith 2005; Zamora & Smith 2008). Rahman *et al.* (2015*a*) carried out CFD simulations of passive and active suspension feeding for the cinctan *P. mansillaensis*, and the results demonstrated there was almost no flow to the mouth

under a passive feeding scenario. Based on this, they inferred that *P. mansillaensis* and all other cinctans were most likely to have been active suspension feeders, with an inhalant current generated by pharyngeal gill slits (as previously proposed; e.g. Smith 2005; Zamora & Smith 2008). Our results for *Gr. ambigua*, *L. barriosensis*, *P. mansillaensis* and *T. bohemicus* at inlet velocities less than 0.30 m/s agree with this, with the very limited flow to the mouth and food grooves pointing towards active suspension feeding as the most plausible feeding mode. However, the strong recirculation of fluid flow to the mouth and food grooves in *Gy. testudiformis*, *U. quadricornuta* and *T. bohemicus* at inlet velocities greater than 0.30 m/s is more consistent with passive suspension feeding on particles transported by ambient currents, which would have been advantageous due to the energetic costs of active pumping (LaBarbera 1984; Vogel 1994). This indicates that cinctans were adapted for different modes of suspension feeding, distributed across phylogeny (Fig. 2). Moreover, the variability in flow patterns observed for *T. bohemicus* (Figs 5E, 6E; Rahman *et al*. 2020, figs S10, S11) suggests that it might have been a facultatively active suspension feeder, switching between passive and active feeding depending on the current velocity, similar to some modern barnacles (Crisp & Southward 1961; Trager *et al*. 1990).

Two potentially important aspects not incorporated into our CFD simulations due to limitations in computing power are the surface roughness of the seafloor and the presence of neighbouring organisms. High surface roughness creates turbulence within the boundary layer, enhancing mixing of nutrients and thereby increasing the availability of food for both passive and active suspension feeders (Denny 1988). However, cinctans lived on soft substrates (Lefebvre & Fatka 2003; Zamora & Álvaro 2010), which would have been characterized by relatively low surface roughness and limited mixing in the boundary layer. The presence of dense communities of epibenthic organisms would also have enhanced turbulence (Denny 1988), but there are no fossil accumulations representing life assemblages of cinctans, and so it is unknown whether individuals lived in close proximity to each other or not.

Our results are suggestive of a trade-off between feeding and stability in cinctans. Taxa with flattened body shapes, such as *Gr. ambigua*, *L. barriosensis* and *P. mansillaensis*, minimized drag and thus enhanced their stability on the seafloor; however, there was almost no flow to the mouth and food grooves, and so they had to expend energy to actively pump water for feeding. In contrast, high-relief forms such as *Gy. testudiformis* and *U. quadricornuta* were much less stable due to the large amounts of drag generated, but they were able to passively direct fluid flow to the mouth and food grooves, thereby feeding more efficiently by relying on ambient water currents. Cinctan phylogeny (Fig. 2) places *Gy. testudiformis* and *U. quadricornuta* in distinct clades, and they independently evolved different strategies for increasing relief to aid passive suspension feeding (a swollen dorsal integument and dorsal projections on marginal plates, respectively). *Trochocystites bohemicus*, which is close to the base of the cinctan tree (Fig. 2), had the best of both worlds; it was characterized by a large but relatively flattened body that reduced the drag coefficient (enhancing stability) and increased flow to the mouth and food grooves (enhancing passive feeding), but only at higher current velocities. However, the apparent advantages provided by the morphology of *T. bohemicus* might have been partly offset by its higher energetic demands; metabolic cost scales as a higher power of mass than energy intake in modern suspension feeders (Sebens 1979, 1982; Sebens *et al*. 2017).

Evolutionary trade-offs, where beneficial changes in a trait are associated with detrimental changes in the same or a different trait, are thought to be pervasive across the tree of life (Agrawal *et al*. 2010). However, demonstrating their existence in fossil taxa has proved challenging, in part due to the difficulties in evaluating functional performance in extinct organisms in a rigorous and quantitative manner. Our results suggest there was an evolutionary trade-off between feeding and stability in Cambrian cinctan echinoderms, with morphological changes that increased the height of the animal inferred to have improved feeding efficiency but reduced stability on the seafloor. Thus, this trade-off points to the creation of multiple locally optimal morphologies in the fitness landscape of cinctans, contributing to the roughness of the landscape (Marshall 2006, 2014). One of the studied species, *T. bohemicus*, deviated from this pattern, indicating that while the trade-off might have been generally true for cinctans, it was not a universal pattern.

CONCLUSION

Our analysis of Cambrian cinctan echinoderms demonstrates that morphology greatly influenced functional performance. Flattened forms (i.e. *Gr. ambigua*, *L. barriosensis* and *P. mansillaensis*) produced lower drag and were more stable on the seafloor, whereas high-relief forms (i.e. *Gy. testudiformis* and *U. quadricornuta*) generated stronger recirculation to the mouth and food grooves, aiding passive suspension feeding. Thus, cinctan functional morphology was partly a trade-off between feeding and stability. This study provides further evidence of the great potential of computational fluid dynamics for

elucidating the function and evolution of ancient organisms (Rahman 2017).

Acknowledgements. This study relied on the work of James O'Shea, who very sadly died in January 2018. James was an outstanding student with enormous potential. He is deeply missed by all who knew him. We thank Andrew Smith for the invitation to submit this article. We are grateful to Brad Deline, Bertrand Lefebvre, Sally Thomas and an anonymous reviewer for their comments on earlier versions of this manuscript. IAR was funded by the Oxford University Museum of Natural History. JO'S was funded by a Palaeontological Association Undergraduate Research Bursary (PA-UB201507). SZ was funded by the Spanish Ministry of Science, Innovation and Universities (CGL2017-87631), co-financed by the European Regional Development Fund and the project 'Aragosaurus: Recursos Geológicos y Paleoambientales' (E18_17R) funded by the Government of Aragon.

Author contributions. IAR and SZ conceived the study. J'OS and SL created 3-D models. IAR carried out CFD simulations. IAR wrote the manuscript with scientific and editorial input from SL and SZ.

DATA ARCHIVING STATEMENT

3-D models and CFD simulation files are available from the Dryad Digital Repository: https://doi.org/10.5061/dryad.12jm63xth

Editor. George Sevastopulo

REFERENCES

AGRAWAL, A. A., CONNER, J. K. and RASMANN, S. 2010. Tradeoffs and negative correlations in evolutionary ecology. 243–268. *In* BELL, M. A., FUTUYMA, D. J., EANES, W. F. and LEVINTON, J. S. (eds). *Evolution since Darwin: The first 150 years*. Sinauer Associates, 688 pp.

ÁLVARO, J. J. and VENNIN, E. 1997. Episodic development of Cambrian eocrinoid-sponge meadows in the Iberian Chains (NE Spain). *Facies*, **37**, 49–64.

BOURKE, J. M., PORTER, W. R., RIDGELY, R. C., LYSON, T. R., SCHACHNER, E. R., BELL, P. R. and WITMER, L. M. 2014. Breathing life into dinosaurs: tackling challenges of soft-tissue restoration and nasal airflow in extinct species. *The Anatomical Record*, **297**, 2148–2186.

CONWAY MORRIS, S. 1998. *The crucible of creation: The Burgess Shale and the rise of animals*. Oxford University Press, 272 pp.

CRISP, D. J. and SOUTHWARD, A. J. 1961. Different types of cirral activity of barnacles. *Philosophical Transactions of the Royal Society B*, **243**, 271–308.

DARROCH, S. A. F., RAHMAN, I. A., GIBSON, B., RACICOT, R. A. and LAFLAMME, M. 2017. Inference of facultative mobility in the enigmatic Ediacaran organism *Parvancorina*. *Biology Letters*, **13**, 20170033.

DAVID, B., LEFEBVRE, B., MOOI, R. and PARSLEY, R. L. 2000. Are homalozoans echinoderms? An answer from the extraxial-axial theory. *Paleobiology*, **26**, 529–555.

DELINE, B., GREENWOOD, J. M., CLARK, J. W., PUTTICK, M. N., PETERSON, K. J. and DONOGHUE, P. C. J. 2018. Evolution of metazoan morphological disparity. *Proceedings of the National Academy of Sciences*, **115**, E8909–E8918.

DENNY, M. W. 1988. *Biology and the mechanics of the wave-swept environment*. Princeton University Press, 329 pp.

DONOGHUE, P. C. J. and PURNELL, M. A. 2009. Distinguishing heat from light in debate over controversial fossils. *BioEssays*, **31**, 178–189.

DYNOWSKI, J. F., NEBELSICK, J. H., KLEIN, A. and ROTH-NEBELSICK, A. 2016. Computational fluid dynamics analysis of the fossil crinoid *Encrinus liliiformis* (Echinodermata: Crinoidea). *PLoS One*, **11**, e0156408.

ERWIN, D. H., LAFLAMME, M., TWEEDT, S. M., SPERLING, E. A., PISANI, D. and PETERSON, K. J. 2011. The Cambrian conundrum: Early divergence and later ecological success in the early history of animals. *Science*, **334**, 1091–1097.

FRIEDRICH, W.-P. 1993. Systematik und Funktionsmorphologie mittelkambrischer Cincta (Carpoidea, Echinodermata). *Beringeria*, **7**, 3–190.

GIBSON, B. M., RAHMAN, I. A., MALONEY, K. M., RACICOT, R. A., MOCKE, H., LAFLAMME, M. and DARROCH, S. A. F. 2019. Gregarious suspension feeding in a modular Ediacaran organism. *Science Advances*, **5**, eaaw0260.

GOULD, S. J. 1989. *Wonderful life: The Burgess Shale and the nature of history*. Norton, 347 pp.

GUTARRA, S., MOON, B. C., RAHMAN, I. A., PALMER, C., LAUTENSCHLAGER, S., BRIMACOMBE, A. J. and BENTON, M. J. 2019. Effects of body plan evolution on the hydrodynamic drag and energy requirements of swimming in ichthyosaurs. *Proceedings of the Royal Society B*, **286**, 20182786.

JEFFERIES, R. P. S., BROWN, N. A. and DALEY, P. E. J. 1996. The early phylogeny of chordates and echinoderms and the origin of chordate left–right asymmetry and bilateral symmetry. *Acta Zoologica*, **77**, 101–122.

JENNER, R. A. and LITTLEWOOD, D. T. J. 2008. Problematica old and new. *Philosophical Transactions of the Royal Society B*, **363**, 1503–1512.

KOEHL, M. A. R. 1976. Mechanical design in sea anemones. 23–31. *In* MACKIE, G. O. (ed.) *Coelenterate ecology and behavior*. Plenum Press, 744 pp.

—— 1984. How do benthic organisms withstand moving water? *American Zoologist*, **24**, 57–70.

—— 1996. When does morphology matter? *Annual Review of Ecology & Systematics*, **27**, 501–542.

LABARBERA, M. 1984. Feeding currents and particle capture mechanisms in suspension feeding animals. *American Zoologist*, **24**, 71–84.

LEFEBVRE, B. and FATKA, O. 2003. Palaeogeographical and palaeoecological aspects of the Cambro-Ordovician radiation of echinoderms in Gondwanan Africa and peri-Gondwanan Europe. *Palaeogeography, Palaeoclimatology, Palaeoecology*, **195**, 73–97.

MARSHALL, C. R. 2006. Explaining the Cambrian "explosion" of animals. *Annual Review of Earth & Planetary Sciences*, **34**, 355–384.

—— 2014. The evolution of morphogenetic fitness landscapes: conceptualising the interplay between the developmental and ecological drivers of morphological innovation. *Australian Journal of Zoology*, **62**, 3–17.

MENTER, F. R. 2009. Review of the shear-stress transport turbulence model experience from an industrial perspective. *International Journal of Computational Fluid Dynamics*, **23**, 305–316.

PARSLEY, R. L. 1999. The Cincta (Homostelea) as blastozoans. 369–375. *In* CANDIA CARNEVALI, M. D. and BONASORO, F. (eds). *Echinoderm research 1998*. Balkema, 550 pp.

PUIG, P., PALANQUES, P. and GUILLÉN, J. 2001. Near-bottom suspended sediment variability caused by storms and near-inertial internal waves on the Ebro mid continental shelf (NW Mediterranean). *Marine Geology*, **178**, 81–93.

RAHMAN, I. A. 2017. Computational fluid dynamics as a tool for testing functional and ecological hypotheses in fossil taxa. *Palaeontology*, **60**, 451–459.

—— and LAUTENSCHLAGER, S. 2017. Applications of three-dimensional box modeling to paleontological functional analysis. 119–132. *In* TAPANILA, L. and RAHMAN, I. A. (eds). *Virtual paleontology*. The Paleontological Society Papers, **22**, 209 pp.

—— and ZAMORA, S. 2009. The oldest cinctan carpoid (stem-group Echinodermata), and the evolution of the water vascular system. *Zoological Journal of the Linnean Society*, **157**, 420–432.

—— —— FALKINGHAM, P. L. and PHILLIPS, J. C. 2015*a*. Cambrian cinctan echinoderms shed light on feeding in the ancestral deuterostome. *Proceedings of the Royal Society B*, **282**, 20151964.

—— DARROCH, S. A. F., RACICOT, R. A. and LAFLAMME, M. 2015*b*. Suspension feeding in the enigmatic Ediacaran organism *Tribrachidium* demonstrates complexity of Neoproterozoic ecosystems. *Science Advances*, **1**, e1500800.

—— O'SHEA, J., LAUTENSCHLAGER, S. and ZAMORA, S. 2020. Data from: Evolutionary trade-off between feeding and stability in Cambrian cinctan echinoderms. *Dryad Digital Repository*. https://doi.org/10.5061/dryad.12jm63xth

RIGBY, S. and TABOR, G. 2006. The use of computational fluid dynamics in reconstructing the hydrodynamic properties of graptolites. *GFF*, **128**, 189–194.

SEBENS, K. P. 1979. The energetics of asexual reproduction and colony formation in benthic marine invertebrates. *American Zoologist*, **19**, 683–697.

—— 1982. The limits to indeterminate growth: an optimal size model applied to passive suspension feeders. *Ecology*, **63**, 209–222.

SEBENS, K., SARÀ, G. and NISHIZAKI, M. 2017. Energetics, particle capture, and growth dynamics of benthic suspension feeders. *In* ROSSI, S., BRAMANTI, L., GORI, A. and OREJAS, C. (eds). *Marine animal forests*. Springer, 1366 pp.

SHIINO, Y., KUWAZURU, O. and YOSHIKAWA, N. 2009. Computational fluid dynamics simulations on a Devonian spiriferid *Paraspirifer bownockeri* (Brachiopoda): generating mechanism of passive feeding flows. *Journal of Theoretical Biology*, **259**, 132–141.

—— —— SUZUKI, Y. and ONO, S. 2012. Swimming capability of the remopleuridid trilobite *Hypodicranotus striatus*: hydrodynamic functions of the exoskeleton and the long, forked hypostome. *Journal of Theoretical Biology*, **300**, 29–38.

SHIMETA, J. and JUMARS, P. A. 1991. Physical mechanisms and rates of particle capture by suspension-feeders. *Oceanography & Marine Biology: An Annual Review*, **29**, 191–257.

SMITH, A. B. 2005. The pre-radial history of echinoderms. *Geological Journal*, **40**, 255–280.

—— 2008. Deuterostomes in a twist: the origins of a radical new body plan. *Evolution & Development*, **10**, 493–503.

—— and ZAMORA, S. 2009. Rooting phylogenies of problematic fossil taxa; a case study using cinctans (stem-group echinoderms). *Palaeontology*, **52**, 803–821.

TRAGER, G. C., HWANG, J.-S. and STRICKLER, J. R. 1990. Barnacle suspension-feeding in variable flow. *Marine Biology*, **105**, 117–127.

UBAGHS, G. 1968. Homostelea. S565–S581. *In* MOORE, R. C. (ed.) *Treatise on invertebrate paleontology. Part S. Echinodermata 1 (2)*. Geological Society of America & University of Kansas, 650 pp.

VALLE-LEVINSON, A. and MATSUNO, T. 2003. Tidal and subtidal flow along a cross-shelf transect on the East China Sea. *Journal of Oceanography*, **59**, 573–584.

VOGEL, S. 1994. *Life in moving fluids*. Princeton University Press, 467 pp.

WARNER, G. F. 1977. On the shapes of passive suspension feeders. 567–576. *In* KEEGAN, B. F., CEIDIGH, P. O. and BOADEN, J. J. S. (eds). *Biology of benthic organisms*. Pergamon Press, 664 pp.

WATERS, J. A., WHITE, L. E., SUMRALL, C. D. and NGUYEN, B. K. 2017. A new model of respiration in blastoid (Echinodermata) hydrospires based on computational fluid dynamic simulations of virtual 3D models. *Journal of Paleontology*, **91**, 662–671.

WROE, S., PARR, W. C. H., LEDOGAR, J. A., BOURKE, J., EVANS, S. P., FIORENZA, L., BENAZZI, S., HUBLIN, J.-J., STRINGER, C., KULLMER, O., CURRY, M., RAE, T. C. and YOKLEY, T. R. 2018. Computer simulations show that Neanderthal facial morphology represents adaptation to cold and high energy demands, but not heavy biting. *Proceedings of the Royal Society B*, **282**, 20180085.

YOUNG, C. M. and BRAITHWAITE, L. F. 1980. Orientation and current-induced flow in the stalked ascidian *Styela montereyensis*. *Biological Bulletin*, **159**, 428–440.

ZAMORA, S. and ÁLVARO, J. J. 2010. Testing for a decline in diversity prior to extinction: Languedocian (latest mid-Cambrian) distribution of cinctans (Echinodermata) in the Iberian Chains, NE Spain. *Palaeontology*, **53**, 1349–1368.

—— and RAHMAN, I. A. 2014. Deciphering the early evolution of echinoderms with Cambrian fossils. *Palaeontology*, **57**, 1105–1119.

—— and SMITH, A. B. 2008. A new Middle Cambrian stem-group echinoderm from Spain: palaeobiological implications of a highly asymmetric cinctan. *Acta Palaeontologica Polonica*, **53**, 207–220.

—— LEFEBVRE, B., ÁLVARO, J. J., CLAUSEN, S., ELICKI, O., FATKA, O., JELL, P., KOUCHINSKI, A., LIN, J.-P., NARDIN, E., PARSLEY, R., ROZHNOV, S., SPRINKLE, J., SUMRALL, C. D., VIZCAÏNO, D. and SMITH, A. B. 2013*a*. Global Cambrian echinoderm diversity and palaeobiogeography. 151–164. *In* HARPER, D. A. T. and SERVAIS, T. (eds). *Early Palaeozoic biogeography and palaeogeography*. Geological Society, London, Memoirs, **38**, 490 pp.

—— RAHMAN, I. A. and SMITH, A. B. 2013*b*. The ontogeny of cinctans (stem-group Echinodermata) as revealed by a new genus, *Graciacystis*, from the middle Cambrian of Spain. *Palaeontology*, **56**, 399–410.

—— DELINE, B., ÁLVARO, J. J. and RAHMAN, I. A. 2017. The Cambrian Substrate Revolution and the early evolution of attachment in suspension-feeding echinoderms. *Earth-Science Reviews*, **171**, 478–491.